SAND79-8634
Unlimited Release

UC-94a

RS-8232-2/52212
C2

The High Temperature Compatibility of Nitrate Salts, Granite Rock and Pelletized Iron Ore

8232-2//052212
00000002 -

V. P. Burolla, J. J. Bartel

Prepared by Sandia Laboratories, Albuquerque, New Mexico 87115 and Livermore, California 94550 for the United States Department of Energy under Contract DE-AC04-76DP00789.

Printed August 1979

Sandia Laboratories

SF 2900 Q(7-73)

Issued by Sandia Laboratories, operated for the United States Department of Energy by Sandia Corporation.

NOTICE

This report was prepared as an account of work sponsored by the United States Government. Neither the United States nor the United States Department of Energy, nor any of their employees, nor any of their contractors, subcontractors, or their employees, makes any warranty, express or implied, or assumes any legal liability or responsibility for the accuracy, completeness or usefulness of any information, apparatus, product or process disclosed, or represents that its use would not infringe privately owned rights.

SAND79-8634
Unlimited Release
Printed August 1979

UC-94a

THE HIGH TEMPERATURE COMPATIBILITY OF NITRATE SALTS, GRANITE ROCK AND PELLETIZED IRON ORE

Victor P. Burolla
Model Labs Division 8424
and
James J. Bartel
Large Power Systems Division 8452
Sandia Laboratories, Livermore CA

ABSTRACT

Under the direction of the Department of Energy, high-temperature (550°C) thermal energy storage concepts are being studied for application with second-generation solar central receiver thermal power systems. This report evaluates the compatibility of the current choice of working fluids with common granite rock and a pelletized iron ore. Results indicate that the long-term stability of iron-ore pellets in binary mixtures of potassium and sodium nitrates is superior to granite rock-salt mixtures and salt systems without solid media. Corrosion of the Inconel 600 vessels was observed.

CONTENTS

	Page
Introduction	9
Procedure	9
Results	11
Discussion	26
Salt-Filler Interactions	26
Salt-Metal Interactions	27
Conclusions	27
References	29

ILLUSTRATIONS

Figure		Page
1.	Vessel Test Assembly	12
2a.	Binary Eutectic Salt Only	13
2b.	Ternary Eutectic Salt and Granite	13
2c.	Binary Eutectic Salt and Pelletized Iron Ore	13
3.	Filler Material After Test	16
4.	Microphotographs of Inconel 600 Vessel Exposed to Salt	18
5.	Microphotographs of Inconel 600 Tube Exposed to Taconite and Salt	19
6.	Microphotographs of Inconel 600 Vessel With Salt and Rocks	20
7a.	Rock Before Exposure (50X)	21
7b.	Rock Before Exposure (200X)	21
8a.	Rock After Salt Exposure (50X)	22
8b.	Rock After Salt Exposure (200X)	22
9a.	Iron Ore Pellet Before Exposure (50X)	23
9b.	Iron Ore Pellet Before Exposure (400X)	23
10a.	Iron Ore Pellet Before Salt Exposure (50X)	24
10b.	Iron Ore Pellet Before Salt Exposure (400X)	24
11.	Pelletized Iron Ore Before and After Exposure	25

TABLES

Table		Page
I.	Materials Tested	10
II.	Test Matrix	11
III.	Summary of Visual Observations	14
IV.	Filler Mass and Salt Melting Point Changes	14
V.	Chemical Analysis Results	15

Introduction

The development of energy storage systems that can be used to generate electricity during periods of low or zero insolation is an important step toward demonstrating the technical and economic viability of solar electric power plants. One technology under consideration by the Department of Energy (DOE) is sensible heat storage with maximum media temperatures ranging from approximately 300°C to 550°C and possibly higher.[1,2] Proposals have included thermocline tanks and dual media storage in which a large portion of the energy would be contained in a stationary, highly porous heat sink. For the lower temperatures, tests have been conducted on several hydrocarbon oils and river gravels to assess their compatibility; however, no test results have been published that evaluate the compatibility of relatively inexpensive filler media such as granite rock or processed iron ore pellets in molten salt mixtures of $NaNO_3$, KNO_3 and $NaNO_2$. The evaluation of these latter combinations, which is the subject of this report, is critical in that the advanced, central receiver large power system conceptual design program (ACR) proposes to use molten salt in the receiver thermal storage system at temperatures to 550°C.

The source, cost, and composition of the materials tested are listed in Table I. Common river gravel, composed mostly of granite, was tested because some storage concepts propose to use salt in either naturally occurring or man-made underground rock caverns or above ground in large metal tanks filled with inexpensive rock to diminish salt volume. Processed iron ore pellets prepared from taconite were proposed as a heat storage media by Honeywell[3]. It is relatively inexpensive ($30-40 per ton at point of manufacture) and more homogeneous and isotropic than most minerals, being approximately 65% iron as α-Fe_2O_3. The selection of Inconel 600 for the test containers was on the basis of its corrosion resistance and potential as a receiver tube material. Ternary eutectic salt mixtures of sodium nitrite ($NaNO_2$), sodium nitrate ($NaNO_3$), and potassium nitrate (KNO_3) can have melting points as low as 142°C, depending on the relative ratios of each constituent. These salts, under the trade name HITEC,® have been used extensively as heat transfer fluids. However, because of the presence of sodium nitrite these mixtures are significantly more expensive than other salts without the nitrite. For this reason, all of the tests reported here except one involved a $NaNO_3$, KNO_3 binary salt mixture (Partherm 430) that melts at 221°C.

Procedure

Five cylindrical vessels were fabricated from Inconel 600 (I-600) tubing (nominal composition by weight 75 % Ni, 15.5 % Cr, 8 % Fe, 0.5 % Mn, 0.25 % Si, 0.08 % C); each vessel was 5.0 cm in diameter and 10 cm long. End caps

® E. I. DuPont

TABLE I

MATERIALS TESTED

Ternary Salt Mixture

Composition:	40 weight percent $NaNO_2$, 7 $NaNO_3$, 53 KNO_3
Supplier:	E. I. DuPont
Melting Point:	142°C (288°F)
Estimated Cost*:	23 cents/lb

Binary Salt Mixture

Composition:	46 weight percent $NaNO_3$, 54 KNO_3
Supplier:	Park Chemical Co.
Melting Point:	220°C (430°F)
Estimated cost*:	13 cents/lb

Granite Rock

Composition:	Potassium Feldspar and Quartz ($KAlSi_3O_8$ and SiO_2) + Other Minerals in Minor Quantities
Supplier:	Owl Rock Co., Barstow, California
Size:	20mm Nominal
Estimated cost*:	$15/ton

Iron Ore Pellets

Composition:	63 weight percent Fe, 28 oxygen in Fe_2O_3, 5 SiO_2, less than 4 P, S, CaO, MgO, H_2O, Mn, Al, all others 1.35%
Supplier:	U.S. Steel, Minnesota
Size:	~12mm Dia Spherical Pellets
Estimated cost*:	$30/ton

*Telephone estimates; considerable variations possible due to local market conditions, transportation cost and quantities.

were fabricated of I-600; one cap was blank and the other was bored with a 6.25 mm O.D. tube attached. After the vessels were loaded with the weighed salt/filler combinations (see Table II), the top cap was welded in place (tungsten inert gas welding). The completed vessel assemblies were then placed horizontally in a muffle furnace with the vent tubes penetrating through the furnace wall (see Figure 1). Each vessel was purged with dry nitrogen gas, and the vent tube was then fitted with a check valve to prevent air entry. The muffle furnace was heated to 550°C, with the temperature controlled and monitored continuously throughout the test.

TABLE II

TEST MATRIX

	TERNARY SALT MIXTURE	BINARY SALT MIXTURE
Granite Rock	Vessel #3	Vessel #1, #2
Iron ore pellets		Vessel #5
No Filler		Vessel #4 (Control)

All five vessels were maintained at 550°C for 700 hours, at which time they were cooled slowly to ambient temperature. The vessels were cut open and the contents removed by remelting the salt when necessary. The rocks and iron ore pellets were first washed with hot water to remove most residual salt, and then dried and weighed. Optical and scanning electron microscopy were used to examine the surface of the rock and taconite pellets, and X-ray diffraction was used to identify the principal iron oxide phase formed in the taconite. The salts were analyzed chemically using emission spectroscopy, atomic absorption, and wet chemical techniques. Melting points of the salt mixtures were determined with a Fischer-Johns melting point apparatus. Metallographic specimens of the I-600 tubing were examined using a scanning electron microscope and energy dispersive X-ray analysis.

Results

The vessels and contents are shown in Figure 2 after opening. The iron ore pellets had changed color from black to brown, and the rock surfaces appeared pitted and encrusted with salt crystals. There was a variation in the salt color from vessel to vessel. In all cases, the color change was from white to various shades of yellow-green, the tint due primarly to the presence of chromium. Table III summarizes the qualitative observations; Table IV displays the changes in filler mass and salt melting points before and after test; and Table V lists the results of the chemical analysis. The iron ore pellets and salt mixture was removed easily from the vessel; in contrast, the salt and rock-salt mixtures were extremely difficult to remove and showed a significant amount of deposition on the wall at the liquid-vapor interface. The post-test filler materials are shown in Figure 3. Degradation

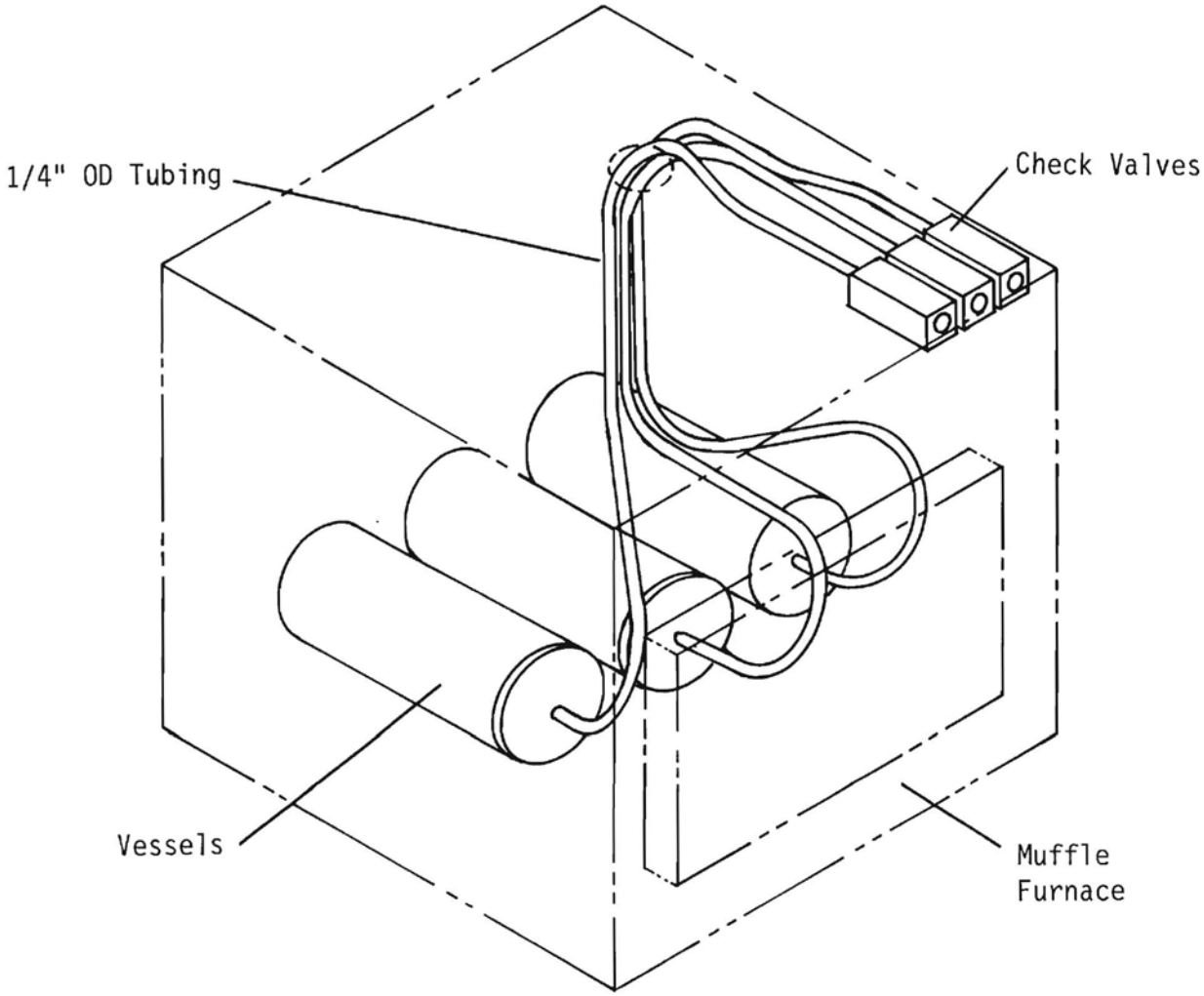

Figure 1. Vessel Test Assembly

Figure 2a. Binary Eutectic Salt Only

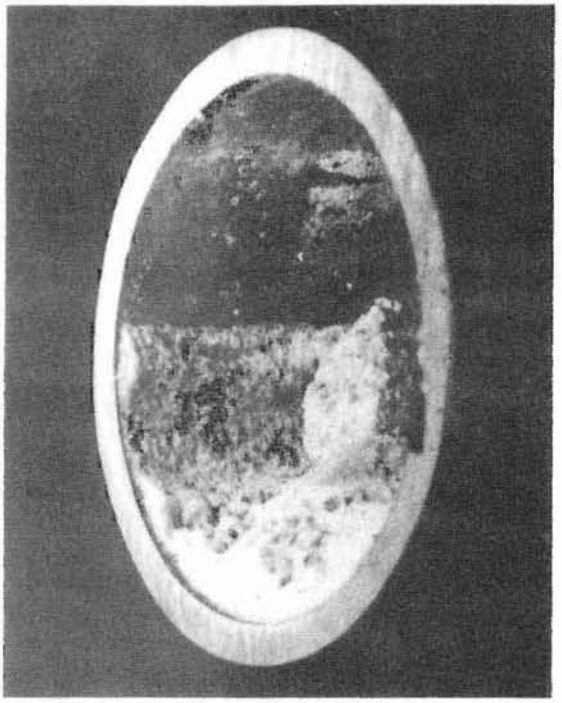

Figure 2b. Ternary Eutectic Salt and Granite

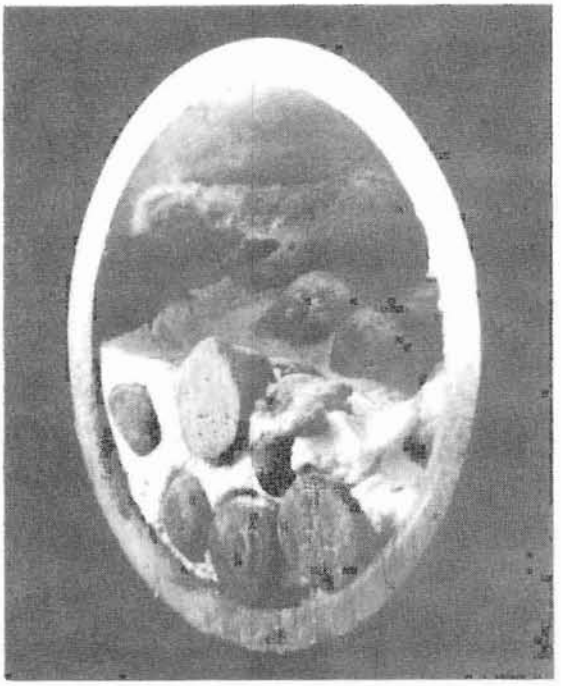

Figure 2c. Binary Eutectic Salt and Pelletized Iron Ore

TABLE III

SUMMARY OF VISUAL OBSERVATIONS

Vessel No.— Contents—	1 & 2 Rock/ Binary Salt	3 Rock/ Ternary Salt	4 Iron Ore Pellets/ Binary salt	5 Control/ Binary salt Only
Deposit on Vessel Walls	Much	Much	None	Some
Surface Changes on Filler	Much	Much	Little	N/A
Adhesion to Vessel Wall	Much	Most	None	Some
Color of Salt	pale green	pale green	very pale green	pale green
Color Separation in Salt	Yes	Yes	No	No
Water Insoluble Precipitates	Much	Most	Little	Negligible

TABLE IV

FILLER MASS AND SALT MELTING POINT CHANGES

Vessel Number	Salt	Filler	Filler Mass(g.) Before	After	%Change	Salt MP.(°C) Before	After	Change
1	Binary*	Rock	200	190	-5	220	190	-30
2	Binary*	Rock	200	182	-9	220	185	-35
3	Ternary†	Rock	200	191	-5	142	180	+38
5	Binary*	Iron Ore	200	218	+9	220	191	-29
4	Binary*	-	-	-	-	220	185	-35

*Binary composition 46 w% $NaNO_3$, 54 KNO_3

†Ternary composition 40 w% $NaNO_2$, 7 $NaNO_3$, 53 KNO_3

TABLE V

CHEMICAL ANALYSIS RESULTS

Vessel No. - Contents -	— Binary	1 Binary + Rock	2 Binary + Rock	5 Binary	4 Binary + Iron Ore	4 Binary + Iron Ore	3 Ternary + Rock
Na^+ (w %)	16.	15.0	15.5	16.6	12.2	12.3	9.6
K^+ (w %)	15.	18.4	18.0	17.9	22.7	19.3	26.3
NO_3^{2-} (w %)	67.	60.6	58.6	47.9	57.6	58.0	46.5
NO_2^{2-} (w %)	0.03	6.9	6.6	12.5	5.83	6.53	17.7
CO_2^{2-} (w %)	0.05	1.3	1.0	0.8	0.1	*	1.0
Ca (ppm)	83	100	100	<1	<1	8	10
Cr (ppm)	5	100	60	600	<1	408	60
Si (ppm)	*	100	200	<1	30	*	10
Al (ppm)	19	60	60	<1	<1	2	3
Fe (ppm)	19	<1	100	200	200	17	<1
Mg (ppm)	81	10	20	1	20	17	<1
Mn (ppm)	4	10	10	20	<10	<1	<10
Ni (ppm)	5	10	10	30	<10	8	<10
Notes:	a	b	b	b	b	c	b

*Not Specifically Determined.

Notes:

[a]All values reported in weight precent determined by wet chemistry, remainder by atomic absorption.

[b]All values reported in weight percent determined by wet chemistry, remainder by emission spectroscopy.

[c]Duplicate analysis

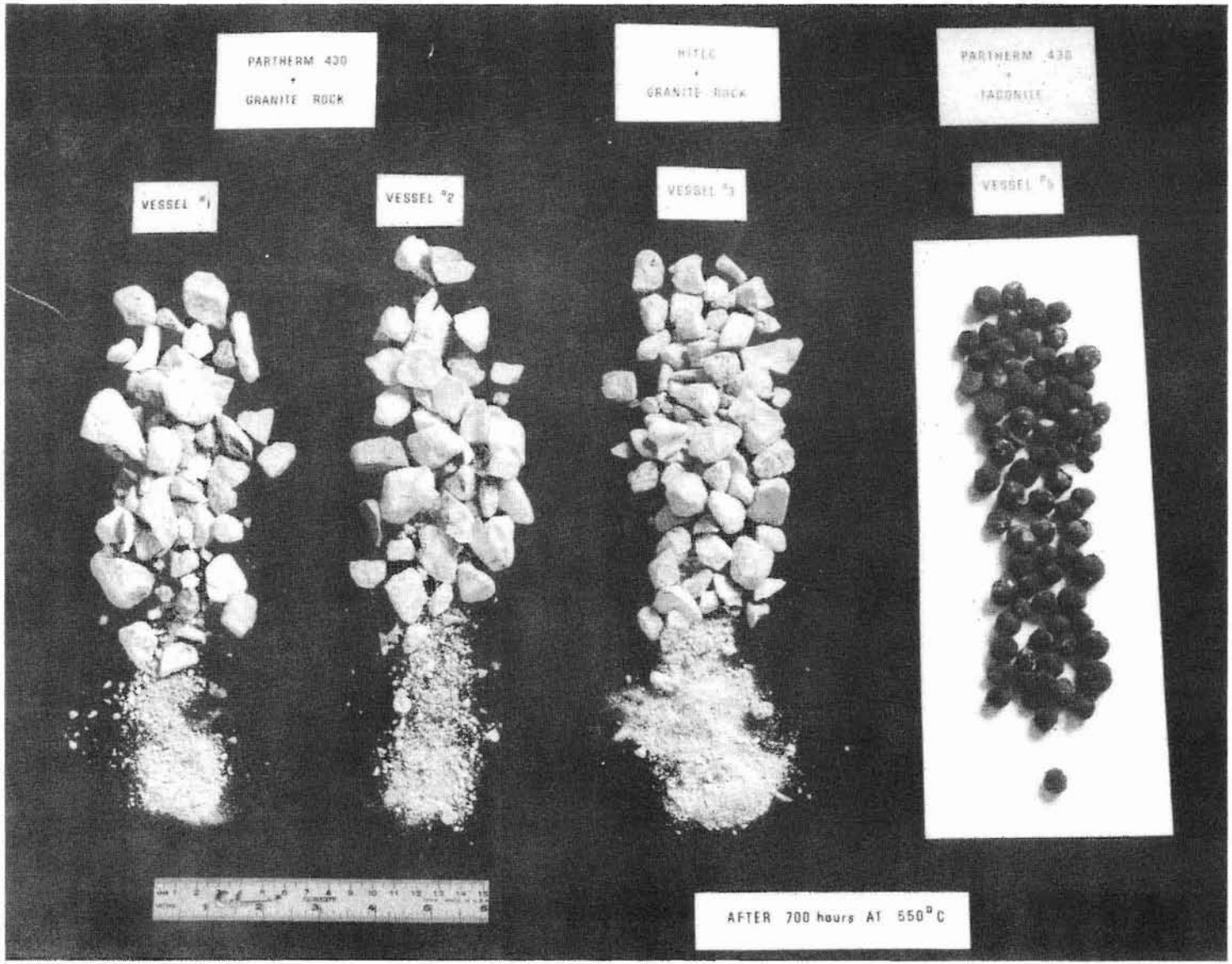

Figure 3. Filler Material After Test

of the granite rock is clearly indicated by the presence of "fines". The iron-ore pellets showed little change other than a change of surface color from black to brown. Scanning electron photomicrographs of vessels and filler media are shown in Figures 4 though 11. A depletion of chromium from the vessel wall in contact with the molten salt is most clearly shown in Figure 5. This is consistent with the increase of chromium concentration found in the salt by chemical analysis (Table V). The surface layer is principally iron, below which a nickel enriched layer is evident. Although not as clearly delineated, similar "layering" of alloy elements is evident in all vessel micrographs.

Figures 7 though 10 show the filler media before and after exposure to the salt. Microphotographs show rounding of surface features; cracks and fissures are evident at the higher magnification. The iron-ore pellet photographs before and after exposure show little change. Figure 11 is a macrophotograph of two iron-ore pellets, one as received and the second after exposure. A white, water insoluble, precipitate was found on several iron-ore pellets; Figure 11 shows the best example. EDAX analysis of the white surface indicated only potassium compounds. Powder diffraction results were inconclusive since the white regions were found to be amorphous.

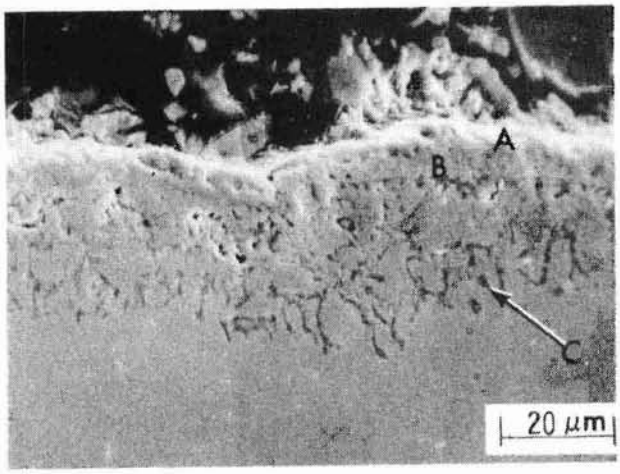

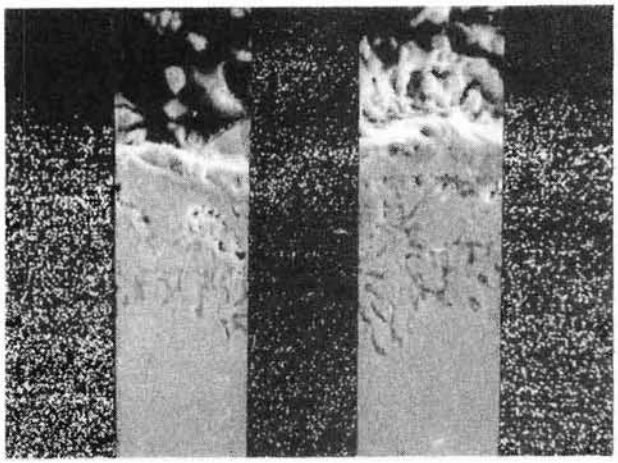

Ni Fe Cr

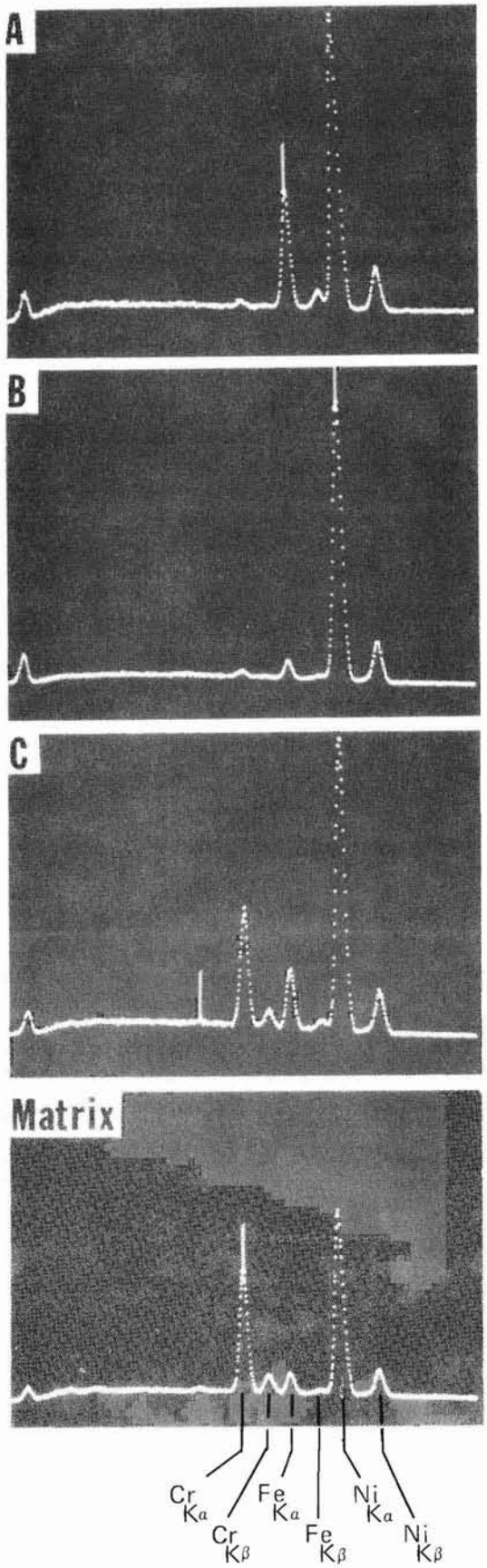

Figure 4. Above, scanning electron photomicrograph of Inconel 600 exposed to binary eutectic salt-granite pelletized rock mix. "A" is surface oxide, principally iron and nickel; "B" is a near surface layer, principally nickel; "C" has slight chromium enrichment in grain boundary regions compared to "Matrix." Directly above are maps of Fe, Ni, and Cr concentrations selectively overlaid on the corresponding regions of the micrograph above. Right, elemental scans.

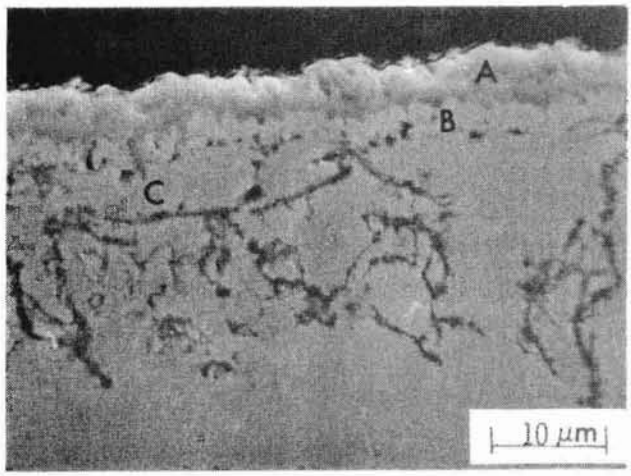

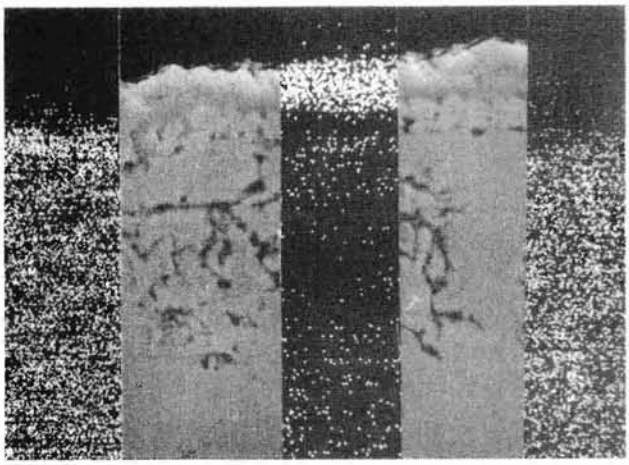

Ni Fe Cr

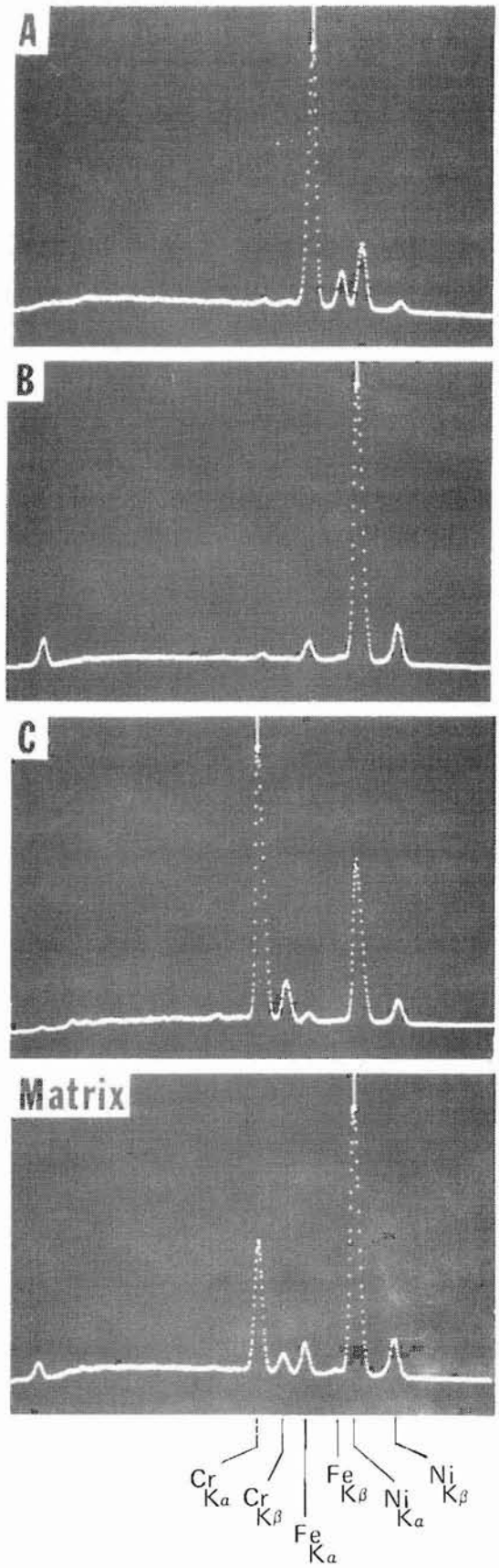

Figure 5. Above, scanning electron photomicrograph of Inconel 600 exposed to binary salt-pelletized iron ore mix. "A" surface oxide, principally iron; "B" subsurface layer, principally nickel; "C" has chromium rich grain boundary regions compared to "Matrix." Directly above are maps of Fe, Ni, and Cr concentrations selectively overlaid on the corresponding regions of the micrograph above. Right, elemental scans.

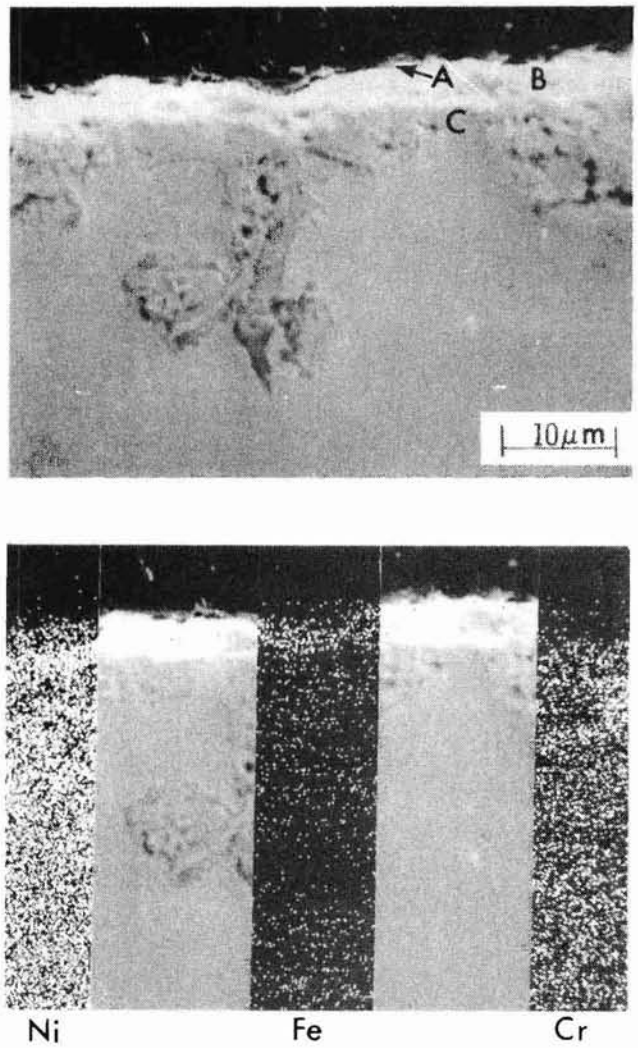

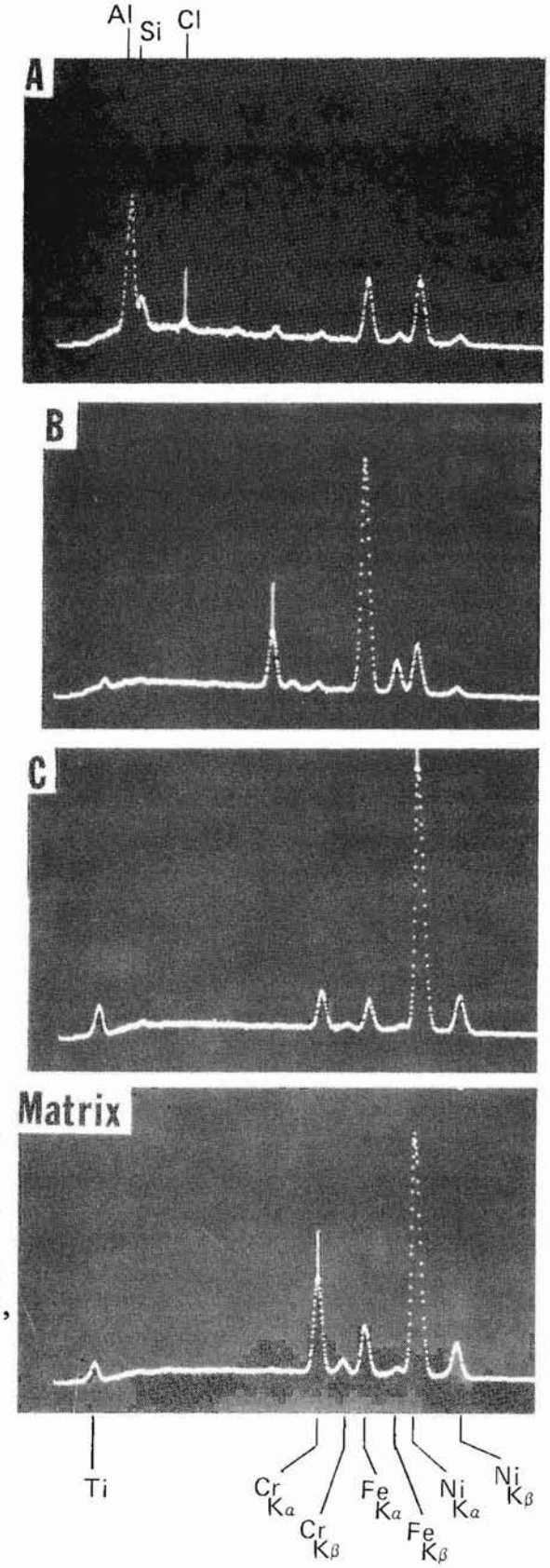

Figure 6. Above, scanning electron photomicrograph of Inconel 600 exposed to binary salt. "A" surface oxide, principally iron and nickel; "B" near surface layer, principally nickel; "C" has slight chromium enrichment in grain boundary regions compared to "Matrix." Directly above are maps of Fe, Ni, and Cr concentrations overlaid on the corresponding regions of the micrograph above. Right, elemental scans.

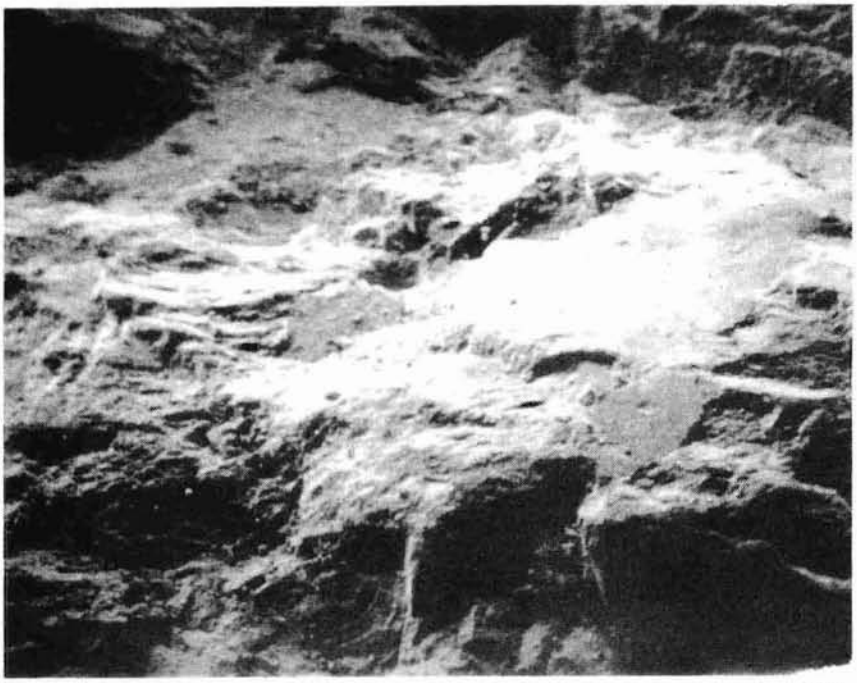

50X

Figure 7a. Rock Before Exposure

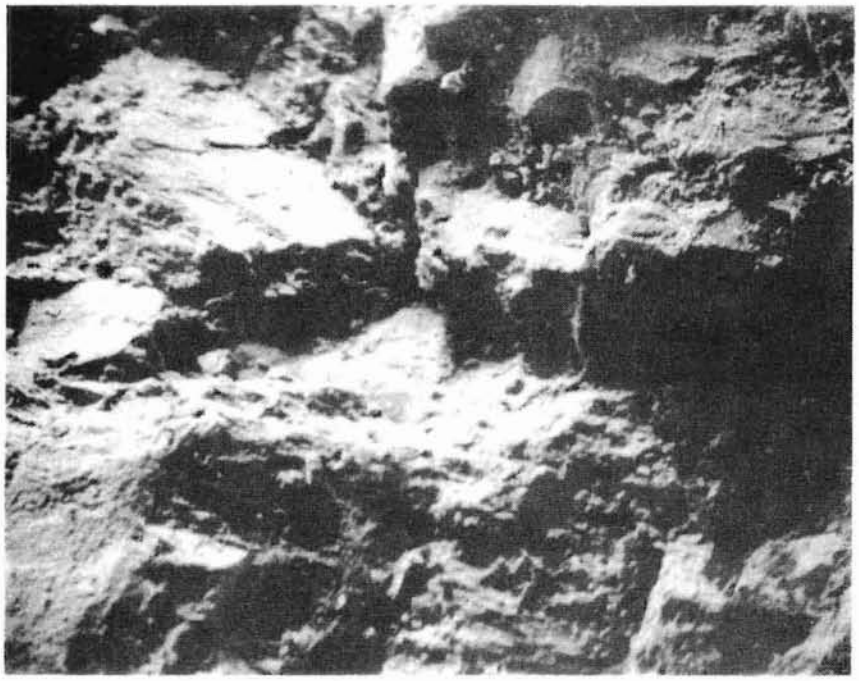

200X

Figure 7b. Rock Before Exposure

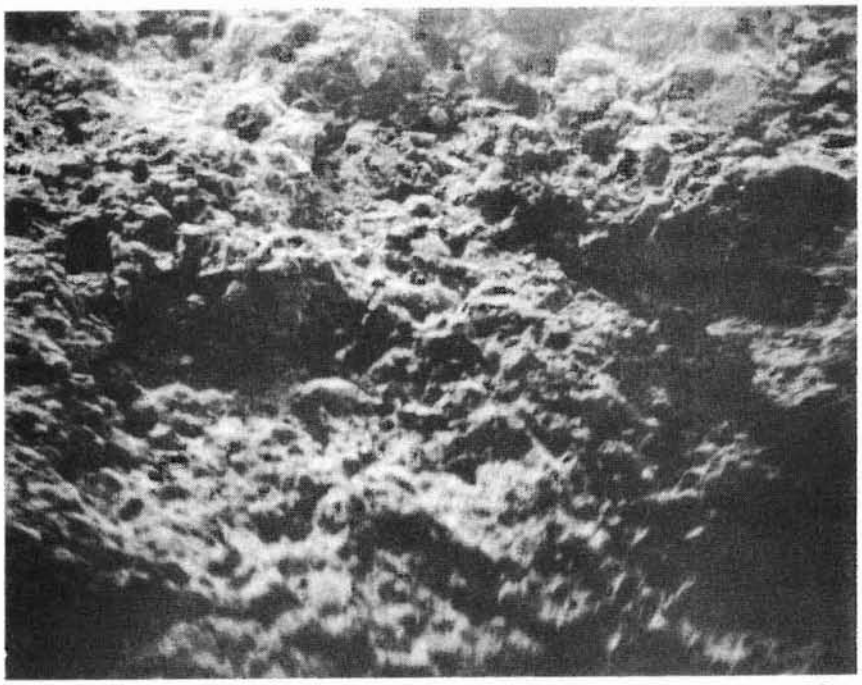

50X

Figure 8a. Rock After Salt Exposure

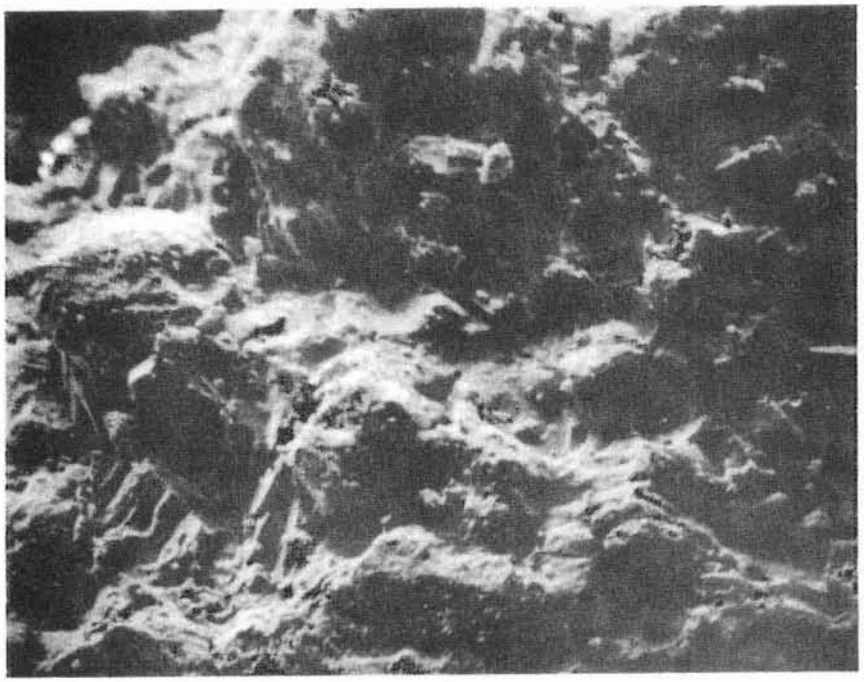

200X

Figure 8b. Rock After Salt Exposure

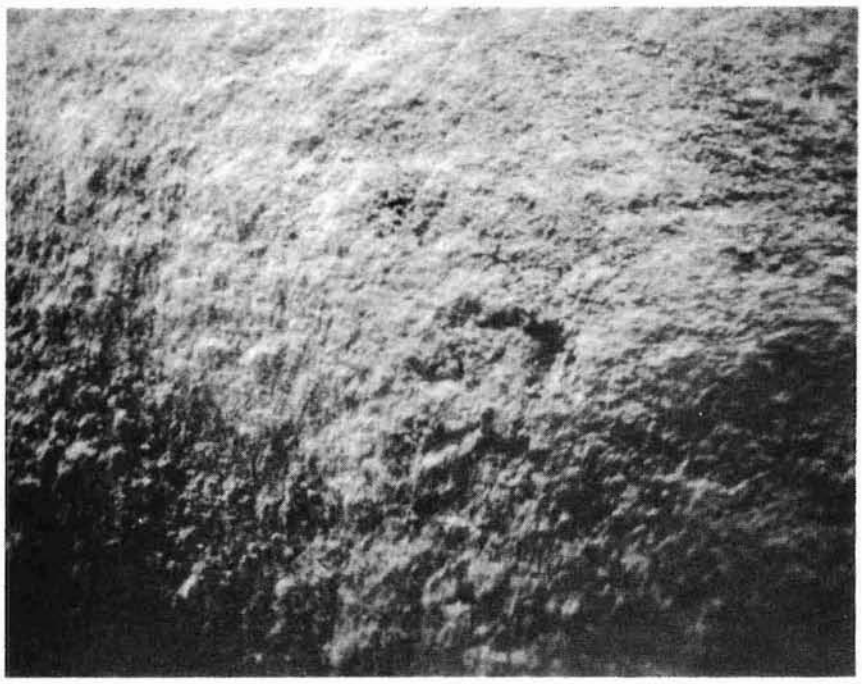

50X

Figure 9a. Iron Ore Pellet Before Exposure

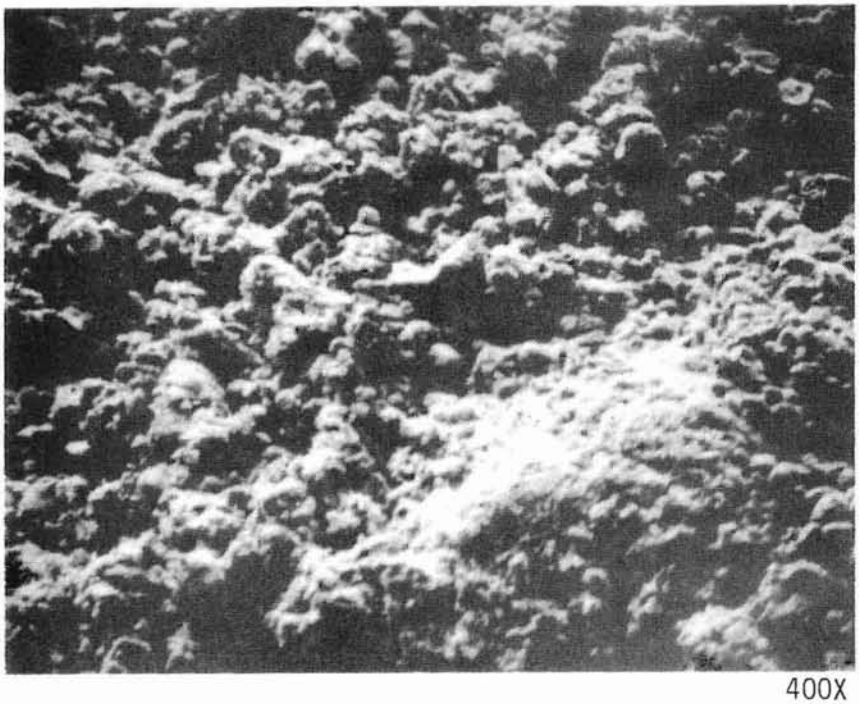

400X

Figure 9b. Iron Ore Pellet Before Exposure

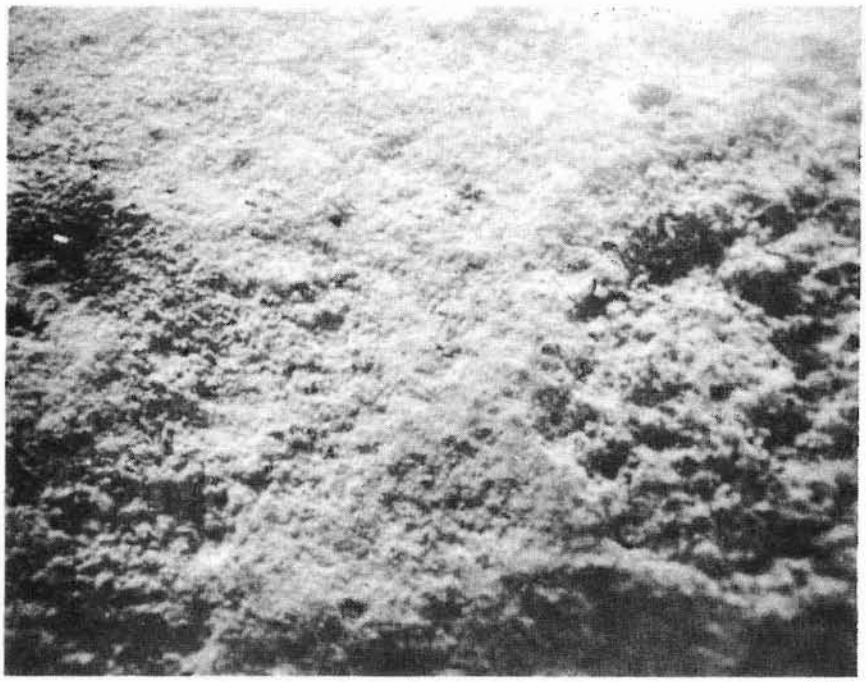

50X

Figure 10a. Iron Ore Pellet After Salt Exposure

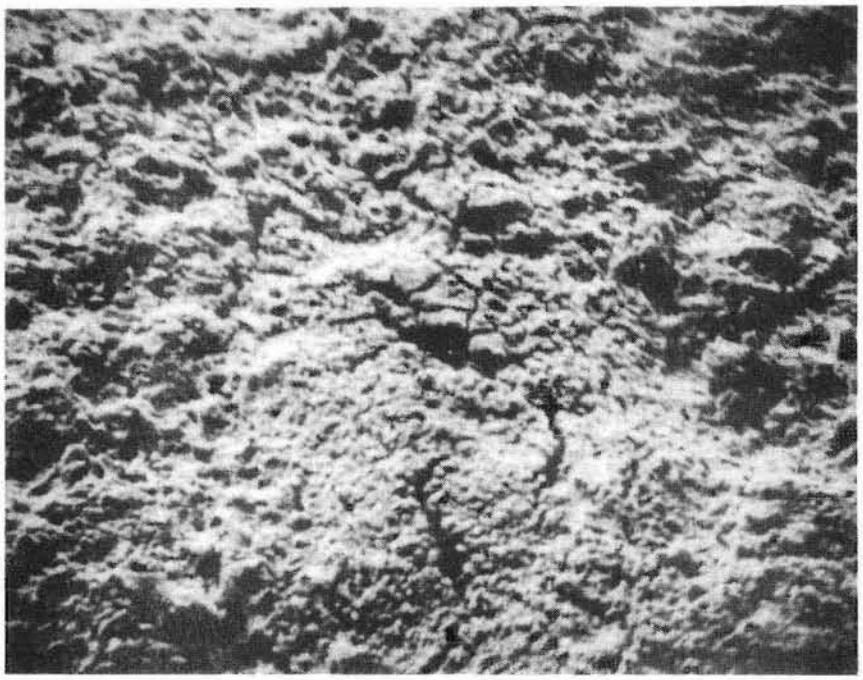

400X

Figure 10b. Iron Ore Pellet After Salt Exposure

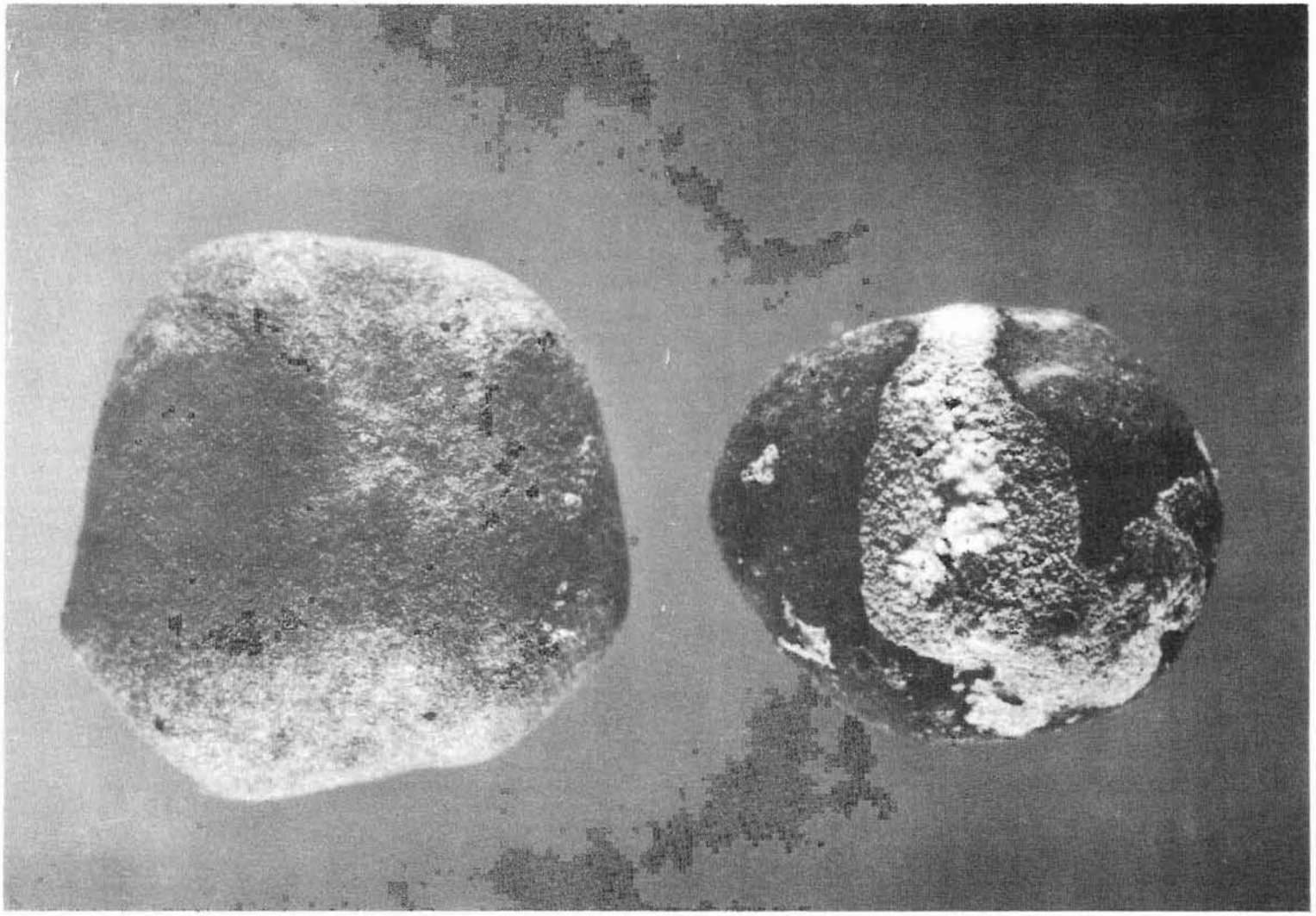

Figure 11. Pelletized Iron Ore Before (left) and After (right) Exposure

Discussion

Salt-Filler Interactions

Based upon the mass change of the granite rock filler media as a result of exposure to the salt, it is apparent that dissolution of the rock occurred. Since granite is composed chiefly of quartz (SiO_2) and potassium feldspar ($KA\ell Si_3O_8$), the formation of Na_2SiO_3 (shown below) has been suggested[5] as a potential dissolution mechanism.

$$2\ NaNO_3\ (\ell) + SiO_2\ (c) \rightleftarrows Na_2SiO_3\ (c) + N_2(g) + \frac{5}{2}\ O_2(g).$$

Other reactions are also possible[6]; for example $2\ NaNO_3 + 2\ SiO_2 \rightarrow Na_2O{\cdot}2\ SiO_2 + N_2 + \frac{5}{2}\ O_2$. The last is thermodynamically favored although it may be reactant limited. Na_2SiO_3 is insoluble in potassium and sodium nitrates[7] but slightly soluble in water;[8] hence it would not have been noticed after the rocks had been washed. Spectroscopic analysis of the solid salt showed significant amounts of aluminum and silicon, which indicates that the feldspar at least dissolves in the molten salt. Further, as shown in Figure 3, the granite rocks were significantly fractured. The fine, sand-like, rock fragments were formed by disintegration and fracture of the 20 mm nominal diameter granite pieces. This fracturing can best be explained by preferrential granular attack of the rocks by the molten salt, since the test involved no thermal cycling.

Some general observations of the salt/rock interactions from microscopic examinations can be made. First, most of the original surface structure of the rock samples was very sharp and angular probably due to exposed grain boundaries (Figure 7). Secondly, the surface structure of exposed rock was much more rounded and pitted; in some instances, remnants of undissolved salt could be seen (Figures 8).

In contrast, the iron ore pellets and salt interacted to a lesser degree. After the test, the pellet filler showed an increase in mass. This increase is due in part to the water insoluble salt decomposition products shown coating the surface of some of the pellets in Figures 3 and 11 and in part to the void volume within the pellets themselves ($\approx$ 18%) which could retain the salt. EDAX analysis of the white surface deposits indicated only potassium compounds were present. (This technique is insensitive to elements with atomic weights less than 20.) In general, the pre- and post-test pellet surfaces showed little difference other than a colar change (Figure 11).

The increase and decrease in the melting points of the ternary and binary salts respectively are consistent with the chemical anlysis and the literature.[8,9] The NO_3^- species can decompose to NO_2^-, which lowers the apparent melting point of the binary; $NaNO_3$ (Nitrate) $\rightleftarrows$ $NaNO_2$ (Nitrite) + $1/2\ O_2$. The oxidation of the nitrate to nitrite raises the apparent melting point of the ternary. There are a multitude of thermodynamic reactions possible; however, it appears that the binary and ternary become chemically similar in long-term use.

Salt-Metal Interactions

As shown in Table V, significant changes occurred in the salt composition and impurities for all test samples. Two analysis were performed on the salt contents of Vessel #5 because the first (spectroscopic) analysis revealed no chromium. A significant amount of chromium was detected in the second analysis, which was consistent with the observed color change of the salt to pale green.

The high chromium concentration in the salt after exposure is consistent with the metallographic results. The near surface oxide layers of all the Inconel 600 specimens examined by X-ray dispersion (Figures 4-6) showed a relative enhancement of iron and depletion of chromium. Figure 5 shows an iron-rich surface layer depleted of chromium immediately below a nickel-rich layer, and finally the bulk matrix material. This material was exposed to the iron ore binary salt combination. For the other combinations, iron enhancement of the surface layer is evident and chromium depletion is indicated by dispersive x-ray results and confirmed by salt chemical analysis. This iron-enriched zone is about 5 μm deep; the corrosion layer is about 20 μm in depth. The nature of the microstructural changes below the iron-enriched zone is unclear; grain boundary attack or internal oxidation are two of several possibilities.

The salt analyses show greater increases in chromium concentration than nickel or iron, which indicates preferential chromium dissolution in the binary eutectic. Systematic variation of chromium concentration through the surface layers has been observed by others on different alloys.[10] Results observed here are consistent. In all the Inconel 600 specimens, the surface layer was tenacious and continuous, with no evidence of spalling.

Conclusions

In comparing all the data presented in this report, the following conclusions were drawn:

1. A thermal storage system employing common granite rock and nitrate salts of potassium and sodium will undergo significant erosion/dissolution of the rock bed in several years time, if operated at or near 550°C. The erosion/dissolution may manufacture increasingly smaller particles that would eventually clog the system and disable it completely.

2. Because of the composition of common granite rock there is the potential for forming significant quantities of insoluble precipitates in a thermal storage system using granite and nitrate salts. These precipitates could not be formed in any meaningful quantities in systems employing taconite pellets, by virtue of their relative purity and composition.

3. There is no evidence to indicate that the erosion of the granite rock is a self-limiting process. What differences in erosion that have been observed are attributed to differences in mineralogical content, and not the formation of a protective coating. There is evidence that erosion of the granite is not limited to the quartz bearing phases.

4. A thermal storage system composed of taconite pellets and nitrate salts of potassium and sodium will maintain the integrity of the taconite bed for many years if operated at 550°C.

5. On a compatibility basis, there is no specific advantage in using HITEC rather than Partherm 430. The rock dissolution rates are the same for both salts, and after 700 hours at 550°C there appears to be virtually no difference in melting points.

REFERENCES

1. Conceptual Design of Advanced Central Receiver Power System Phase 1, Martin Marietta, Sept. 1978.

2. Status Report on the Direct Absorption Receiver, SAND78-8702, T. D. Brumleve, July 1978

3. Solar Pilot Plant, Phase 1, Preliminary Design Report, Vol. 5, Honeywell Inc., May 1977.

4. Principles of Geology, 3rd Ed., J. Gilluly, A. C. Waters and A. O. Woodford, W. H. Freeman and Company, 1968.

5. Personal communication with Dr. Stanley Cantor, Oak Ridge National Laboratory, August 17, 1977, with Reference to: A) JANAF Thermochemical Tables, NSTDS-NBS 37, B) K. H. Stern, J. Phys. Chem. Ref. Data, 1, (3),768 (1972) and C) K. K. Kelly, U. S. Bureau of Mines Bulletin 584.

6. C. M. Kramer, personal communication.

7. Handbook of Chemistry and Physics, 59th Ed., Robert C. Weast, Editor, Chemical Rubber Co., 1978, p. D-83.

8. J. Alexander, Jr., and S. G. Hindin, "Phase Relations in Heat Transfer Salt Systems" Ind. and Engrg. Chem. 39 (8), Aug 1947, 1044-1049.

9. E. G. Bohlman, Heat Transfer Salt for High Temperature Steam Generation, Oak Ridge National Laboratory, ORNL. TM. 377-7, December, 1972.

10. C. M. Kramer, W. H. Smyrl, and W. B. Estill, Corrosion of Fe Alloys in HITEC at 823K, SAND78-8256, February, 1979.

UNLIMITED RELEASE

INITIAL DISTRIBUTION:

TIC/UC94a (257)

USDOE
Division of Energy Storage Systems
Washington, D. C. 20545
Attn: G. Pezdirtz

USDOE/STOR
Advanced Physical Methods
Washington, D. C. 20545
Attn: J. H. Swisher

USDOE
Chemical and Thermal Storage Branch
Washington, D. C. 20545
Attn: J. Gahimer

USDOE
Albuquerque Operations Office
Special Programs Division
P.O. Box 5400
Albuquerque, NM 87115
Attn: D. K. Nowlin

NASA-Lewis Research Center (3)
Cleveland, OH 44101
Attn: W. J. Masica
J. Calogeras
L. H. Gordon

Oak Ridge National Laboratory (2)
Oak Ridge, TN 37830
Attn: H. H. Hoffman
S. Cantor

USDOE (4)
San Francisco Operations Office
1333 Broadway
Oakland, CA 94612
Attn: J. Blasy
R. Hughey
D. Elliott
L. Prince

USDOE (5)
Division of Solar Technology
Washington D. C. 20545
Attn: G. W. Braun
L. Melamed
M. U. Gutstein
G. M. Kaplan
J. E. Rannels

Aerospace Corporation
2350 El Segundo Blvd.
Attn: E. Katz

JPL (2)
4800 Oak Grove Dr.
Pasadena, CA 91103
Attn: V. Truscello
R. Turner

EPRI (2)
P.O. Box 10412
3412 Hillview Ave.
Palo Alto, CA 94303
Attn: J. Bigger
T. R. Schneider

SERI (4)
1536 Cole Blvd.
Golden, CO 80401
Attn: J. C. Grosskreutz
C. J. Bishop
R. Copeland
B. Butler

R. N. Schweinberg
DOE-STMPO
9650 Flair Park Drive
El Monte, CA 91731

Honeywell Systems and Research
Center Aerospace Defense Group
Minneapolis, MN 55413
Attn: R. LeFrois (T301)

Martin Marietta Aerospace
Denver Division
P.O. Box 179
Denver, CO 80201
Attn: T. Heaton

McDonnell Douglas Corporation (2)
5301 Bolsa Avence
Huntington Beach, CA 92647
Attn: R. Hallet
R. Holl

Rockwell International
Rocketdyne Division
6633 Canoga Avenue
Canoga Park, CA 91304
Attn: J. Friefeld

C. Winter, 4000
J. H. Scott, 4000
G. E. Brandvold, 4710; Attn: R. H. Braasch, 4715
D. G. Schueler, 4719
J. A. Leonard, 4721
J. R. Banas, 4722
A. Narath, 5000

V. L. Dugan, 4720
H. M. Stoller, 4730
R. S. Claassen, 5800; Attn: G. Kepler, 5810
M. J. Davis, 5830
H. J. Saxton, 5840

K. B. Wischmann, 5811
R. E. Whan, 5820
H. J. Rack, 5832
F. P. Gerstle, Jr., 5844
T. B. Cook, Jr., 8000
W. E. Alzheimer, 8120; Attn: C. S. Hoyle, 8122
R. J. Gallagher, 8124
A. N. Blackwell, 8200

B. F. Murphey, 8300
D. M. Schuster, 8310; Attn: D. R. Adolphson, 8312
W. R. Hoover, 8314
L. A. West, 8315
J. C. Swearengen, 8316

R. W. Mar, 8313
C. Kramer, 8313
R. W. Bradshaw. 8313
D. A. Nissen, 8313
D. B. Dawson, 8314

S. L. Robinson, 8314
T. S. Gold, 8320; Attn: P. J. Eicker, 8326
L. Gutierrez, 8400
C. Selvage 8420
V. Burolla, 8424 (20)
R. C. Wayne, 8450
T. T. Bramlette, 8451
T. D. Brumleve, 8451
W. G. Wilson, 8451
L. Radosevich, 8452
J. J. Bartel, 8452 (20)
A. C. Skinrood, 8452
J. D. Gilson 8453
W. S. Winters, 8453

F. J. Cupps, 8265/Technical Library Processes Division, 3141
Technical Library Processes Division, 3141 (2)
Library and Security Classification Division, 8266-2 (3)

Org.	Bldg.	Name	Rec'd by*	Org.	Bldg.	Name	Rec'd by*

*Recipient must initial on classified documents.